MARS CRATER DEPTH-SIZE-FREQUENCY DISTRIBUTION: ANALYSIS OF CRATER DEPTH-AGE CONNECTION. William Bruckman[1] , and Abraham Ruiz[1] ; [1]University of Puerto Rico At Humacao, Department of Physics, Call Box 860,Humacao,Puerto Rico,00792(miguelwillia.bruckman@upr.edu)

We have investigated the relation between impact craters number vs. their rim to floor depth, de, and diameter, D, using the Robbins et al Mars global database [1]. We were able to approximately reproduce the data with the simple formula (Figures (1) and (2)) :

$$\boldsymbol{N}(D, de) \approx \boldsymbol{N}(D, 0)\,[1-x]^2 \ , \qquad 1$$

$$N_{nor} \ \equiv \ \boldsymbol{N}(D, de)/\boldsymbol{N}(D, 0) \approx [1-x]^2 \ , \qquad 2$$

where $\boldsymbol{N}(D, de)$ represents the number of craters, per diameter bin, with depth $> de$, and

$$x \equiv de/demax \quad . \qquad 3$$

For craters with diameters 8, 16, and 32 kilometers (km) the expression $demax$ used above is given by the following Boyce et al [2] formula for the deepest freshest Martian craters :

$$demax = 0.381 D^{0.52} \quad . \qquad 4$$

However for diameters of 64 and 80 km, the above D exponent is slightly modified to 0.51 and 0.50, respectively. We argue, at the end of the abstract, that the above approximate parabolic behavior, in Eq.(2), could be a consequence of the potential energy involved in crater degradation.

$\boldsymbol{N}(D, 0)$ is the total number of craters, including all depths. This function was described in previous works [3, 4], where it was found that

$$\boldsymbol{N}(D, 0) = N = \bar{\Phi}\tau_{\text{mean}}\,\{1 - Exp[-\tau_f/\tau_{mean}]\}, \qquad 5$$

$$\bar{\Phi}\tau_{\text{mean}} = \frac{1.43x10^5}{D^{1.8}}\,, \qquad 6$$

$$\tau_f/\tau_{mean} = \frac{2.48x10^4}{D^{2.5}} \approx (57/D)^{2.5}\,, \qquad 7$$

$$\bar{\Phi} = \left(\frac{1}{\tau_f}\right)\int_0^{\tau_f} \Phi\, d\tau = \left(\frac{1}{\tau_f}\right)\frac{3.55x10^9}{D^{4.3}}. \qquad 8$$

The analytical model above, Eqs. (5)-(8), gives the craters population as a function of crater diameter, D, and was justified by taking into consideration the reduction in crater number as a function of time, caused by the elimination of craters due to effects such as erosion, obliteration by other impacts, and tectonic changes. The model was applied, in references [3,4] (Figure 3) to Mars Barlow's impact crater catalog [5], explaining very well the data, for $D > \sim 8km$, and the presence of two well-defined slopes in the $\log[N]$ vs $\log[D]$ plot, of -4.3 and -1.8, corresponding to the asymptotic limits

$$N = \bar{\Phi}\tau_f = \frac{3.55x10^9}{D^{4.3}}; \qquad \tau_f/\tau_{mean} \ll 1,\ D \gg 57km,$$

$$N = \bar{\Phi}\tau_{mean} = \frac{1.43x10^5}{D^{1.8}},\ \tau_f/\tau_{mean} \gg 1, D \ll 57km.$$

Nevertheless, some numerical modifications would be needed to adapt the above equations to the data in [1], but the main ideas and conclusions remain, with the following dynamical interpretation: $\bar{\Phi}(D)$ is the time average (over the total time of craters formation τ_f) of the rate of meteorite impacts per diameter bin, $\Phi(D)$, capable of forming craters of diameter D. Also, τ_{mean} is the mean-life of craters of diameter D, since it can be shown [3,4] that $Exp[-\tau/\tau_{mean}]$ is the fraction of craters surviving today, that were formed at time τ ago (hence, 1- $Exp[-\tau/\tau_{mean}]$ is then the fraction that disappeared). We can interpret the above formalism in a statistical or probabilistic manner. Thus, for instance, $\bar{\Phi}$ can be viewed as the probability of impacts per unit time, while $1/\tau_{mean}$ represents the probability, per unit time, for a crater to disappear. Accordingly, Eq.(5) is therefore the familiar formula describing the evolution in time of N, resulting from these production vs. destruction processes.

From Eq.(7) we see that $\tau_{mean}\alpha\, D^{2.5} \approx D^2\, demax$, and, furthermore, we can express the volume, V, of a pristine crater as $V = kD^2\, demax$, where k depends on the specific of the geometry of the crater. Thus we have the interesting result that $\tau_{mean} \approx \alpha\, V$, which is a simple and sensible relation that explains the observations.

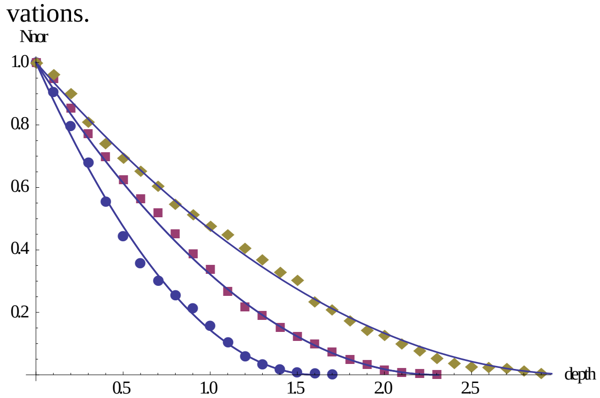

Figure 1

$Plot\ N_{nor}\ vs.de(km);$

$D = 16km\ (blue), 32km(red), 64km(orange).$

Data from Ref [1], curves from Eq.(2) parabola.

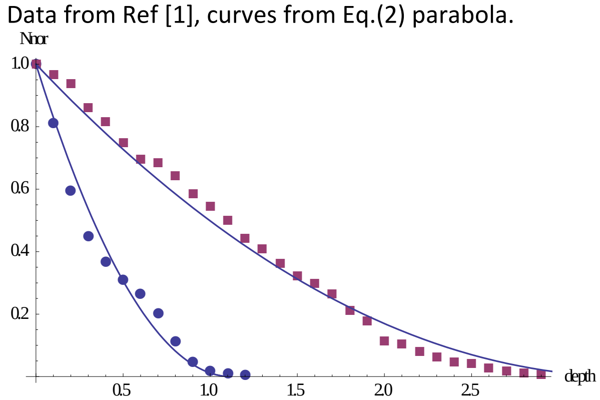

Figure 2

$Plot\ N_{nor} vs.de(km); D = 8km\ (blue), 80km(red).$

Data from Ref [1], curves from Eq.(2) parabola.

Formula (4), for the deepest freshest Martian craters, can be interpreted in the following way. When an impact crater, of diameter$D$, is formed, its initial depth is determined probabilistically by Eq. (4). This interpretation is suggested in the depth vs. diameter plots illustrated in Boyce et al and Robbins et al papers, where the number of craters sharply drops to zero when depths are larger than certain $demax$ value, given by Eq. (4). Moreover, this sharp reduction in number can be explained if the statistical deviation from the most probable maximum depth, $\Delta(demax)$, is small compared with $demax$.

In an idealistic model, where craters of diameter D and initial depth = $demax$ degrade uniformly, reducing their depth at the same rate, we can then associate a physical age τ, corresponding to a crater depth = de, so that larger τ implies lower de. Thus, in such heuristic situation, counting all craters, $\boldsymbol{N}(D, de)$, deeper than de (depth$>de$) gives also the number of craters younger than τ ($N(D,\tau)$). However, in a realistic model, where differences in degradation rate are expected, the number $\boldsymbol{N}(D, de)$ would only be an approximation to the actual $N(D,\tau)$. In other words, a crater with depth $> de$ is only probabilistically younger than craters with depth $< de$. Nevertheless, we still expect that $\boldsymbol{N}(D, de)$ is similar to $N(D,\tau)$, and therefore in what follows we will investigate the implications of the assumption $\boldsymbol{N}(D, de) \approx N(D,\tau) = \bar{\Phi}\tau_{\text{mean}}\,\{1 - Exp[-\tau/\tau_{mean}]\}$, where now, representing $N(D,\tau)$, we are using Eq.(5) with τ replacing τ_f.

In Figure (2), for $D = 8km$ and $80km$, we see larger discrepancies between the data and the parabolic approximation in Eq.(2), than in Figure (1) (a situation that exist also for $D > 80km$). On the other hand, the region of applicability of Eq. (4) [2] is $12km < D < 49km$, consequently, from now on we will restrict the analysis for craters in this region. In this case $\boldsymbol{N}(D, 0) \approx N = \bar{\Phi}\tau_{mean}$ is a good approximation, corresponding to the slope - 1.8 in the left part of Figure (3). Then, $\boldsymbol{N}(D, de) \approx N(D,\tau)$, imply $N_{nor} \approx [1-x]^2 \approx 1 - Exp[-\tau/\tau_{mean}]$, or , solving for τ: $\tau/\tau_{mean} \approx -\ln[1-y^2]$, $y \equiv 1 - x$. N_{nor} means the fraction of craters, of diameter D, with depth larger than de, while, on the other hand, $1 - Exp[-\tau/\tau_{mean}]$ is the fraction of craters, created at τ, that disappeared during the time τ.

We argue below that the fractional potential energy associated with the filling up of a crater, thus lowering x, behaves similarly to $N_{nor} \approx [1-x]^2 \equiv y^2$. To that end, consider the assumption that craters mostly degrade by deposited material from the bottom up so that $z \equiv y\, demax$, then measures by how much the original crater floor if lifted from $z = 0$. Hence, when a crater floor is raised from z to $z + dz$ there is an additional mass, dm, with a corresponding potential energy change $dU =$(dm)$gz = (\rho A dz)gz$, where ρ and A are the density and the area cross section of dm, respectively, and g is the acceleration of gravity; thus we have:
$dN_{nor} \approx d(y^2) = 2ydy = 2\, dU/(\rho Ag[demax]^2)$.
Furthermore, we expect that the changes in z occur without altering much D, and hence A is approximately constant. Therefore $N_{nor} \approx dU/U_{max}$, where $U_{max} = {}^1\!/_2\,(\rho Ag[demax]^2)$, and consequently $N_{nor} \approx U/U_{max}$. Moreover, since N_{nor} is also approximately equal to the fraction of craters, formed at τ, that disappeared during the time τ, the above result is suggesting that the parabolic behavior is a consequence of the potential energy involved in transforming craters.

In conclusion we have , in Eqs.(1) to (8), a two dimensional (depth and diameter) analytical representation of Mars craters number $\boldsymbol{N}(D, de)$, which is a good approximation, particularly for $12km \le D \le 49km$ (slope -1.8 in Figure (3)), to the Robbins et al [1] data. This result was also interpreted in terms of a statistical relation between age τ and the depth of craters. Potential energy associated to crater evolution is also discussed for physical insight.

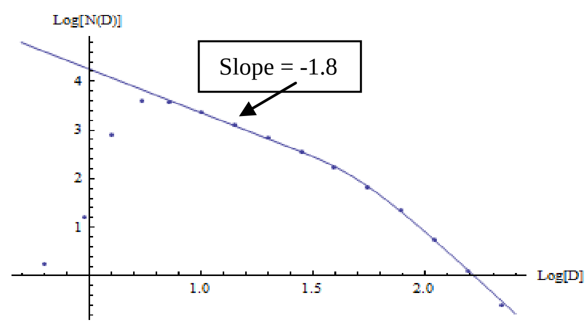

Figure 3: Log-Log $Plot$ of number of craters per bin, $\boldsymbol{N}(D)$ vs D(km), based on Barlow's Mars catalog, and the curve from the model in Eqs. (5) to (8). Data for $D < \sim 8km$ is undercounted.

References:

[1]Robbins, S.J., and B.M. Hynek (2012), A new global database of Mars impact craters $\ge 1\ km.$, Database creation properties and parameters, J. Geophys. Res., 117, E05004.
[2]Boyce, Joseph M. ; Garbeil, Harold (2007), Geophysical Research Letters, Volume 34, Issue 16.
[3]Bruckman W., Ruiz A.,Ramos E. .,(2004),arxiv pdf.astro-ph/0402051.
[4]Bruckman W., Ruiz A.,Ramos E. .,(2013),arxiv pdf.astro-ph/1212.3273.
[5]Barlow, N.G. (1988), Crater size-frequency distribution and a revised Martian relative chronology, Icarus, 75, 285.-305.